

VLBI Astrometry of the Semiregular Variable RX Bootis

Tatsuya KAMEZAKI¹, Akiharu NAKAGAWA¹, Toshihiro OMODAKA¹, Tomoharu KURAYAMA¹, Hiroshi IMAI¹, Daniel TAFOYA¹, Makoto MATSUI¹, Yoshiro NISHIDA¹, Takumi NAGAYAMA², Mareki HONMA², Hideyuki KOBAYASHI², Takeshi MIYAJI², Mine TAKEUTI³

¹*Department of Physics and Astronomy, Graduate School of Science and Engineering, Kagoshima University, 1-21-35 Korimoto, Kagoshima 890-0065, Japan*

²*Mizusawa VLBI Observatory, Mitaka Office, National Astronomical Observatory of Japan, 2-21-1 Osawa, Mitaka, Tokyo 181-8588, Japan*

³*Astronomical Institute, Tohoku University, 6-3 Aramaki, Aoba-ku Sendai, Japan 980-8578
kamezaki@milkyway.sci.kagoshima-u.ac.jp*

(Received 2010 July 12; accepted 2011 August 11)

Abstract

We present distance measurement of the semiregular variable RX Bootis (RX Boo) with its annual parallax. Using the unique dual-beam system of the VLBI Exploration of Radio Astrometry (VERA) telescope, we conducted astrometric observations of a water maser spot accompanying RX Boo referred to the quasar J1419+2706 separated by $1^\circ.69$ from RX Boo. We have measured the annual parallax of RX Boo to be 7.31 ± 0.50 mas, corresponding to a distance of 136_{-9}^{+10} pc, from the one-year monitoring observation data of one maser spot at $V_{\text{LSR}} = 3.2 \text{ km s}^{-1}$. The distance itself is consistent with the one obtained with Hipparcos. The distance uncertainty is reduced by a factor of two, allowing us to determine the stellar properties more accurately. Using our distance, we discuss the location of RX Boo in various sequences of Period-Luminosity (PL) relations. We found RX Boo is located in the Mira sequence of PL relation. In addition, we calculated the radius of photosphere and the mass limitation of RX Boo and discussed its evolutionary status.

Key words: stars: AGB and post-AGB — stars: individual(RX Bootis) — stars: late-type

1. Introduction

In some kinds of variable stars, there is relations between the absolute magnitudes and the variation periods. This is called the Period-Luminosity (PL) relation. PL relations of long

period variable stars (for example, Miras or Semi-Regular Variable stars (SRVs)) have long been investigated since they were found in Large Magellanic Cloud (LMC) (Glass & Evans 1981; Feast et al. 1989; Groenewegen & Whitelock 1996; Wood 2000; Cioni et al. 2001; Ita et al. 2004; Noda et al. 2004). When we use PL relation, we can estimate absolute magnitudes using periods. With these absolute magnitudes and apparent magnitudes from observations, we can calculate distances of these stars. Detailed study of PL relations has given the multiplicity of the relation usually explained by the difference in excited pulsation mode. For the red long-period variable stars, such a multiplicity is first reported by Wood (2000).

Although PL relations in our galaxy are studied (Whitelock & Feast 2000; Zijlstra et al. 2002; Knapp et al. 2003; Yeşilyaprak & Aslan 2004; Glass & van Leeuwen 2007; Whitelock et al. 2008), more studies will be required to establish the precise relation. In the case of LMC, we can study PL relations by using apparent magnitudes on assumption that all variable stars in LMC have the same distances, since the thickness of LMC is much smaller than the distance to LMC. On the other hand, it is obvious that variable stars in our galaxy have large relative difference in distances. To determine more precise PL relations in our galaxy, we need to obtain distances and apparent magnitudes for more variable stars. So, we measured the distance from annual parallax using a VLBI method.

Among long-period variable stars, RX Bootis (RX Boo) is one of the most interesting star because the star has two different periods (Taylor 1987; Andronov & Kudashkina 1988; Mattei et al. 1997; Speil 2006) and classified as SRb group which show low amplitude and less regular variability than Miras or SRa group. It is known that regular and high amplitude variables are found on a common PL relation for our galaxy and LMC (e.g. Whitelock et al. (2008)). It is interesting whether or not the positions of RX Boo situate on the PL sequence of Miras. The study of the parallax of RX Boo will be useful to clarify the nature of SRb group.

We performed astrometric observations with the VLBI Exploration of Radio Astrometry (VERA). VERA is a Japanese VLBI array dedicated to phase referencing VLBI observations (Kobayashi et al. 2003). It consists of four antennas (Mizusawa, Iriki, Ogasawara and Ishigakijima). VERA can measure annual parallaxes and proper motions of many astronomical objects at 22 and 43 GHz. With the dual-beam system of VERA, we observe target and reference sources simultaneously. The system makes it possible to cancel out the effect of atmospheric fluctuations between two sources (Honma et al. 2008a).

Winnberg et al. (2008) monitored RX Boo over twenty years with single-dish observations using Effelsberg 100-m and Medicina 32-m telescopes. They also observed water masers in RX Boo using the Very Large Array (VLA) on four occasions in the period from 1990 to 1992 and later in 1995. Then they revealed the distribution of water masers around RX Boo. They detected the emission of incomplete shell around RX Boo. The inner radius of the shell is estimated to be 15 AU. They conclude that the variability of water masers around RX Boo is due to the appearance and disappearance of maser clouds with a lifetime of ~ 1 year. With

Table 1. Observation dates

| epoch | Date | Year/DOY | antenna [†] | $\Delta V(\text{kms}^{-1})^{\ddagger}$ |
|-------|------------------|----------|----------------------|--|
| 1 | 2008 February 19 | 2008/037 | 4 | 0.42 |
| 2* | 2008 May 1 | 2008/121 | 4 | 0.21 |
| 3* | 2008 June 11 | 2008/162 | 4 | 0.21 |
| 4* | 2008 July 16 | 2008/197 | 4 | 0.21 |
| 5* | 2008 November 11 | 2008/315 | 4 | 0.21 |
| 6* | 2008 December 8 | 2008/342 | 4 | 0.21 |
| 7* | 2009 January 10 | 2009/010 | 3 | 0.42 |
| 8* | 2009 February 4 | 2009/035 | 4 | 0.21 |
| 9* | 2009 March 12 | 2009/071 | 3 | 0.42 |
| 10* | 2009 May 5 | 2009/125 | 4 | 0.42 |
| 11 | 2009 September 5 | 2009/248 | 4 | 0.42 |
| 12 | 2009 October 3 | 2009/276 | 4 | 0.42 |

* Observations used in the estimation of annual parallax.

† Total number of antennas joined the VLBI observation.

‡ Velocity resolution of the maser IF for each observation.

infrared interferometers, the angular diameter of RX Boo is estimated as 18.4 ± 0.5 mas and 21.0 ± 0.3 mas in K band ($2.2 \mu\text{m}$) and L' band ($3.8 \mu\text{m}$), respectively, with the model of uniform disks (Dyck et al. 1996; Chagnon et al. 2002). We can convert these apparent sizes to actual sizes by using distance. RX Boo emits SiO and OH masers as well as water masers (Boboltz & Claussen 2004; Szymczak et al. 1995). The annual parallax of RX Boo was measured to be 6.42 ± 1.00 mas by Hipparcos (Perryman et al. 1997). From CO observations, Olofsson et al. (2002) estimated its mass-loss rate and expansion velocity of $6 \times 10^{-7} M_{\odot} \text{yr}^{-1}$ and 9.3kms^{-1} , respectively. Teyssier et al. (2006) also obtained the values of $2 \times 10^{-7} M_{\odot} \text{yr}^{-1}$ and 7.5kms^{-1} from CO observations.

In this paper, the observations and data reduction are described in section 2. In section 3, we present the annual parallax of RX Boo. Finally, in section 4, we discuss the PL relations and stellar properties of RX Boo.

2. Observations and data reduction

2.1. VLBI observations

We conducted monthly VLBI observations of water masers from February 2008 to October 2009 with VERA. We show the observation dates in Table 1. The duration of each observation was typically 8 hours, yielding an on-source integration time of 5 to 6 hours. Synthesized beam size (FWHM) was typically $1.2 \text{mas} \times 0.6 \text{mas}$.

To obtain positions of maser spots around RX Boo, we observed a continuum source J1419+2706 simultaneously as a position reference. The phase tracking center of RX Boo and J1419+2706 are $(\alpha_{J2000.0}, \delta_{J2000.0}) = (14^{\text{h}}24^{\text{m}}11^{\text{s}}6206, +25^{\circ}42'12''909)$ and $(\alpha_{J2000.0}, \delta_{J2000.0}) = (14^{\text{h}}19^{\text{m}}59^{\text{s}}2971, +27^{\circ}06'25''5530)$, respectively. The separation angle between two sources is $1^{\circ}69$. In three observations, we did not detect any maser spot due to the bad weather conditions or the time variation of maser emission. Among twelve epochs, we used nine epochs that we detected a maser spot for the estimation of the annual parallax. In the seventh observation in 2009 January, Iriki station did not participate. In the ninth observation in 2009 March, Ogasawara station did not participate. The shape of the synthesized beam of ninth observation is different from those of the other observations. Data recording rate of 1024 Mbps was adopted with the VERA DIR2000 recording system, which yields a total bandwidth of 256 MHz with 2-bit digitization. The 256 MHz data of left-hand circular polarization were divided into 16 IFs which had bandwidth of 16 MHz. One IF is used to receive the maser emission and the others are used to receive the continuum emission from J1419+2706. The correlation was carried out with Mitaka FX correlator (Shibata et al. 1998) at National Astronomical Observatory of Japan (NAOJ). The rest frequency of 22.235080 GHz is adopted for water maser emission. The velocity resolution (ΔV) of the maser IF for each observation is also shown in table 1. In six observations, the IF assigned to the water maser was divided into 512 spectral channels, yielding a frequency resolution of 31.25 kHz, corresponding to a velocity resolution of 0.42 km s^{-1} . In the other observations, the maser IFs have bandwidths of 8 MHz. They were divided into 512 spectral channels, yielding a frequency resolution of 15.625 kHz and a velocity resolution of 0.21 km s^{-1} . For the data of J1419+2706, each IF channel was divided into 64 spectral channels in all observations. This corresponds to the velocity resolution of 3.37 km s^{-1} .

2.2. Calibration and Imaging

We analyzed VLBI data with Astronomical Imaging Package Software (AIPS) developed by National Radio Astronomical Observatory (NRAO). We conducted the amplitude calibration using the system noise temperature recorded in each station during observations. In the process of fringe search of the reference source J1419+2706, we solved group delays, phases, and delay rates at intervals of 30 seconds using a task FRING with integration times of 2–3 minutes. We transferred these solutions to the data of RX Boo with a task TACOP and calibrated the visibilities. We also transferred the phase and amplitude solutions derived from self-calibration of J1419+2706 and applied them to the data of RX Boo.

Since the a-priori delay tracking model of the correlator is not sufficiently accurate for high-precision astrometry, the recalculation of the tracking using a better model with CALC3/MSOLV (Jike et al. 2005; Manabe et al. 1991) were made after the correlation. We must correct delay- and phase-differences between the model of the correlator and the better

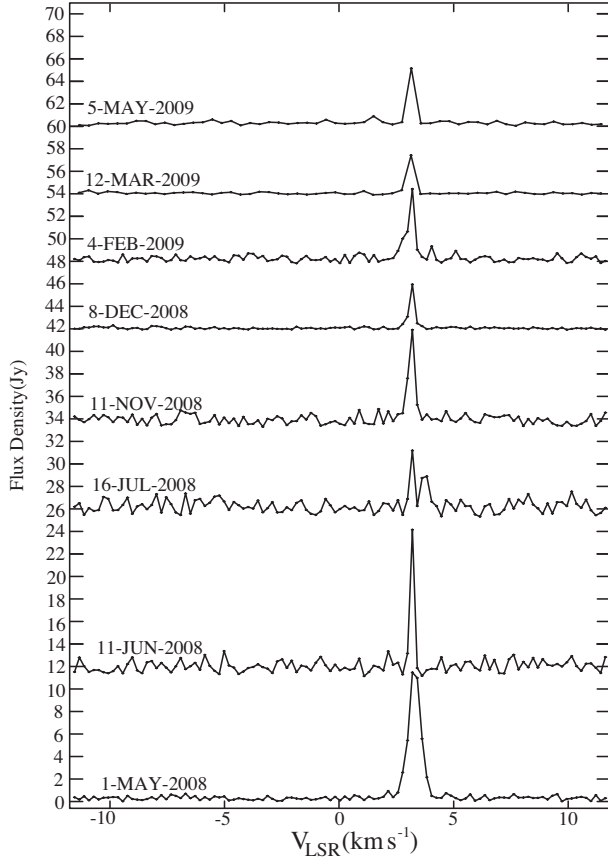


Fig. 1. The time variation of the cross-power spectra of RX Boo obtained by VLBI observations at 22 GHz with VERA. This spectra were obtained from the baseline of Mizusawa – Iriki. We cannot show the spectrum in the 7th epoch on 2009 January 10, because Iriki station did not joined the VLBI observation.

model. By multiplying the delay differences and observation frequencies, the delay differences were converted to phase differences. These delay- and phase-differences were loaded into AIPS with a task TBIN and applied to the visibility data. Note that the better model includes the effect of the wet atmosphere of Earth measured by the Global Positioning System (GPS) at each station (Honma et al. 2008b).

To accomplish the phase referencing analysis between the target maser and continuum reference source, we calibrated phases and delay offsets derived from the differences of signal path lengths between two receivers (Honma et al. 2008a).

As a result of these calibration, we obtained the time variation of cross-power spectra of RX Boo as shown in figure 1. From this figure, we found the LSR velocity of the peak did not change among our VLBI observations. This component was $V_{\text{LSR}} = 3.2 \text{ km s}^{-1}$ and had been strong before our observations, as seen in Winnberg et al. (2008).

Finally, the calibrated visibilities were Fourier transformed to make synthesized images using a task IMAGR. Several frequency channels at which we detected masers were imaged. Obtained images of water masers at a LSR velocity of 3.2 km s^{-1} are shown in figure 2. Using a

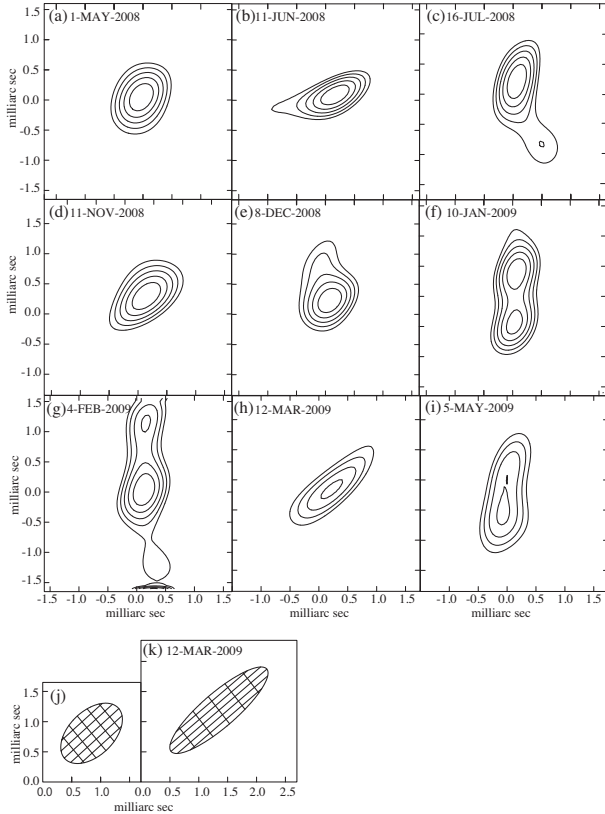


Fig. 2. (a–i) Contours of masers in each epoch at a channel of $V_{\text{LSR}} = 3.2 \text{ km s}^{-1}$. The center of each map is shown in table 2. (j) Synthesized beam in the 8th epoch on 2009 February 4. The shapes of the other epochs except the 9th epoch on 2009 March 12 are almost same. (k) Synthesized beam in the 9th epoch on 2009 March 12.

task IMFIT, we fitted the image of each frequency channel to two-dimensional Gaussian models for obtaining the positions of the maser spots.

3. Results

3.1. Uncertainty of each epoch

It is very important to determine the position error of each epoch because it affects the fitting for the annual parallax of RX Boo. So, we explain the position error of each epoch before least square analysis for the annual parallax. The position error of each measurement was estimated from the root sum square of the following three error factors: (1) the airmass effect σ_A , (2) the errors in station positions σ_S , and (3) the quality of images σ_I . After the calibration of airmass effect in the delay tracking model, there still remains an uncertainty of about 3 cm in the zenith direction (Nakagawa et al. 2008; Honma et al. 2007). Therefore, the error from factor (1) is estimated to be $\sigma_A = 80\text{--}110 \mu\text{as}$ (Nakagawa et al. 2008; Honma et al. 2007). Station positions are determined to be an accuracy of $\sim 3 \text{ mm}$ based on geodetic observation (Nakagawa et al. 2008; Honma et al. 2007), the error from factor (2) was estimated

Table 2. parameters of a detected maser spot in each epoch

| epoch | $\Delta\alpha \cos\delta[\text{mas}]^*$ | $\sigma_{\Delta\alpha \cos\delta}[\text{mas}]^\dagger$ | $\Delta\delta[\text{mas}]^*$ | $\sigma_{\Delta\delta}[\text{mas}]^\dagger$ | $S[\text{Jy beam}^{-1}]^\ddagger$ | SNR |
|-------|---|--|------------------------------|---|-----------------------------------|-------|
| 2 | 0.00 | 0.11 | 0.00 | 0.11 | 6.4 | 25.95 |
| 3 | -0.52 | 0.12 | -5.43 | 0.12 | 2.3 | 14.32 |
| 4 | -2.03 | 0.15 | -5.75 | 0.15 | 4.8 | 11.29 |
| 5 | 14.93 | 0.14 | -34.18 | 0.14 | 3.6 | 16.92 |
| 6 | 20.02 | 0.12 | -38.10 | 0.12 | 6.2 | 21.33 |
| 7 | 23.91 | 0.11 | -41.48 | 0.11 | 2.1 | 14.92 |
| 8 | 26.03 | 0.13 | -43.85 | 0.13 | 2.0 | 14.59 |
| 9 | 28.28 | 0.29 | -49.64 | 0.29 | 0.8 | 8.41 |
| 10 | 24.56 | 0.26 | -44.84 | 0.26 | 3.4 | 5.38 |

* Right Ascension and declination offsets from $(\alpha_{J2000.0}, \delta_{J2000.0}) = (14^{\text{h}}24^{\text{m}}11^{\text{s}}.6206, +25^{\circ}42'12''.906)$.

† Position errors in right ascension and declination.

‡ Peak fluxes of the maser spots.

to be $\sigma_S = 8\mu\text{as}$. We estimate the error from factor (3) from $\sigma_I = \theta_b/\text{SNR}$, where θ_b is a root sum square of major and minor axes of the synthesized beams and SNR is a signal-to-noise ratio in the phase referenced image of the maser. Because SNR was affected by observational condition and intensity variation of the maser, the error was estimated to be $\sigma_I = 50\text{--}250\mu\text{as}$. Thus, the error of each observation was estimated to be $110\text{--}300\mu\text{as}$ by taking root sum squares of these factors. The errors are shown in table 2 and figure 3 and 4 as the error bars. In addition to these three error factors, we can consider error raised by maser structure. This error factor is smaller than $110\text{--}300\mu\text{as}$ of $\sigma_{\Delta\alpha \cos\delta}$ or $\sigma_{\Delta\delta}$. In table 2, there are positions, errors in the positions, peak Intensity S and SNRs of detected maser spot in each epoch, where positions are relative offsets from the position of the maser in the 2nd epoch.

3.2. Least square analysis for the annual parallax

In order to obtain the annual parallax, we adopted the assumptions that the maser spot has no acceleration and the reference source is fixed on the sky.

We conducted the weighted least square fitting analysis. Its weights are based on the position errors. The error in each epoch is shown in table 2. To calculate the parallax, we used maser spots which have sufficient signal-to-noise ratios on the phase-referenced images ($\text{SNR} > 5$). Only one maser spot with $V_{\text{LSR}} = 3.2\text{kms}^{-1}$ is selected with this criterion. We performed the least square fitting by using the following equations ;

$$\Delta\alpha \cos\delta = \varpi(-\sin\alpha \cos\lambda_{\odot} + \cos\epsilon \cos\alpha \sin\lambda_{\odot}) + (\mu_{\alpha} \cos\delta)t + \alpha_0 \cos\delta \quad (1)$$

$$\Delta\delta = \varpi(\sin\epsilon \cos\delta \sin\lambda_{\odot} - \cos\alpha \sin\delta \cos\lambda_{\odot} - \cos\epsilon \sin\alpha \sin\delta \sin\lambda_{\odot}) + \mu_{\delta}t + \delta_0 \quad (2)$$

where $(\Delta\alpha \cos\delta, \Delta\delta)$ are the displacements of the observed maser spot, $(\mu_{\alpha} \cos\delta, \mu_{\delta})$ are the

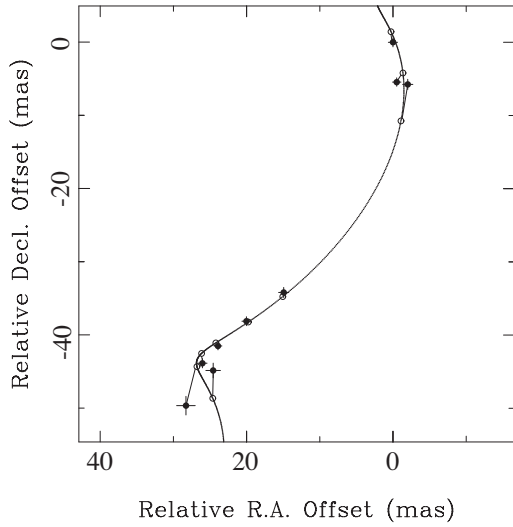


Fig. 3. Relative position of the maser spot around RX Boo with respect to the phase tracking center $((\alpha, \delta) = (14^{\text{h}}24^{\text{m}}11^{\text{s}}.6206, +25^{\circ}42'12''.909))$. Filled circles with error bars indicate the observed positions. Open circles indicate the positions calculated from the least square fitting.

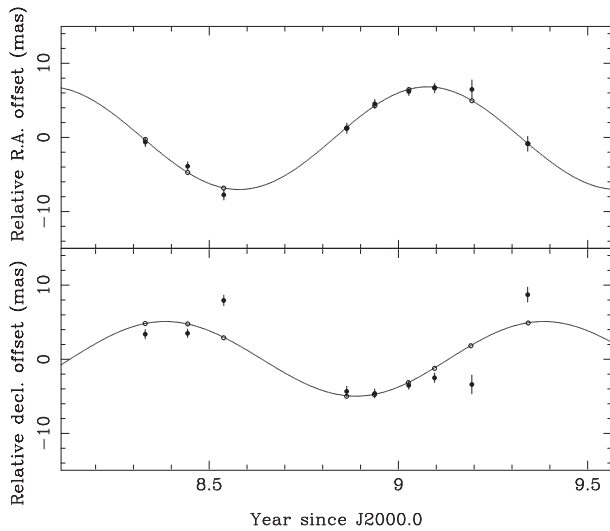


Fig. 4. Time variation of the position of a maser spot around RX Boo in right ascension (top) and declination (bottom) after subtracting the linear proper motion. The solid line is the fitting result of the annual parallax. Filled circles with error bars indicate the observed positions. Open circles indicate the positions calculated from the least square fitting.

linear motions of the maser around RX Boo, t is time, ϖ is the annual parallax, (α, δ) are the right ascension and declination of the source, λ_{\odot} is ecliptic longitude of the Sun, ϵ is the obliquity of the ecliptic and (α_0, δ_0) is the right ascension and the declination when $t = 0$. In this fitting, we derived five parameters; $\varpi, \mu_{\alpha} \cos \delta, \mu_{\delta}, \alpha_0$ and δ_0 . The total number of data is eighteen (right ascension and declination of nine epochs).

In figure 3 and 4, we showed observed positions and results of the fitting. In figure 3, we

present the motion of one maser spot with $V_{\text{LSR}} = 3.2 \text{ km s}^{-1}$ with respect to the phase tracking center. In figure 4, parallactic motion in right ascension and declination are presented. The apparent motion clearly shows an effect of parallactic motion. Based on the least square fitting analysis, the annual parallax was determined to be $7.31 \pm 0.50 \text{ mas}$, corresponding to the distance of $136_{-9}^{+10} \text{ pc}$. The proper motion of the spot was $(\mu_{\alpha} \cos \delta, \mu_{\delta}) = (24.55 \pm 1.06 \text{ mas yr}^{-1}, -49.67 \pm 2.38 \text{ mas yr}^{-1})$.

3.3. Comparison with previous results

Table 3. our results and Hipparcos' results

| | Our result | Hipparcos* |
|---------------------------------------|---------------------------------------|---------------------------------------|
| ϖ^{\dagger} | $7.31 \pm 0.50 \text{ mas}$ | $6.42 \pm 1.00 \text{ mas}$ |
| $\mu_{\alpha} \cos \delta^{\ddagger}$ | $24.55 \pm 1.06 \text{ mas yr}^{-1}$ | $21.74 \pm 0.90 \text{ mas yr}^{-1}$ |
| μ_{δ}^{\ddagger} | $-49.67 \pm 2.38 \text{ mas yr}^{-1}$ | $-49.70 \pm 0.49 \text{ mas yr}^{-1}$ |

* Data from Perryman et al. (1997)

† Annual parallax.

‡ proper motions.

Here, we compare our results with previous results. In table 3, our results and Hipparcos' results are summarized. In comparison with Hipparcos' parallax, $\varpi_{\text{HIP}} = 6.42 \pm 1.00 \text{ mas}$, our parallax is consistent with the Hipparcos' parallax. According to Hipparcos' result, the proper motion of RX Boo is $(\mu_{\alpha} \cos \delta, \mu_{\delta}) = (21.74 \pm 0.90 \text{ mas yr}^{-1}, -49.70 \pm 0.49 \text{ mas yr}^{-1})$. In the declination component, the proper motion from our analysis is consistent with the result from Hipparcos, but in the right ascension component, the motion is 2.81 mas yr^{-1} larger than Hipparcos' result. This difference of the proper motions between Hipparcos' and ours corresponds to 1.8 kms^{-1} at the distance of RX Boo. We think that this is the velocity of the maser motion with respect to the star itself. From CO observations, the LSR velocity of the star is 1.0 kms^{-1} (Teyssier et al. 2006). The difference of the LSR velocities between the star and the water maser is 2.2 kms^{-1} . The difference of the proper motions between Hipparcos' and ours is almost as large as that of the LSR velocities between the star and the water maser. The difference of the proper motions between Hipparcos' and ours may be caused by the motion of the maser spot with respect to the star itself.

From the directions of the proper motion and the radial velocity, we can know the positional relationship between the maser and star. The proper motion of the maser with respect to the central star is $(\mu_{\alpha} \cos \delta, \mu_{\delta}) = (2.81 \text{ mas yr}^{-1}, 0.03 \text{ mas yr}^{-1})$ and directs the position angle of $89^{\circ}4$. The position angle of the maser is $89^{\circ}4$ with respect to the central star. We expect that this maser is located in east direction for the central star. This is consistent with the result of VLA (Winnberg et al. 2008) and their detected masers which had the similar radial velocity distributed in the same direction.

Table 4. Period of RX Boo

| Periods (days) | | Reference |
|----------------|------------|------------------------------|
| Short Group | Long Group | |
| 160.0 | 302.0 | Taylor (1987) |
| 179.1, 164.0 | 352.0 | Andronov & Kudashkina (1988) |
| 162.3 | 304.7 | Mattei et al. (1997) |
| | 340.0 | previous version of GCVS |
| 159.6 | 278.0 | Speil (2006) |
| 162.3 | | GCVS (Samus et al. (2009)) |

Winnberg et al. (2008) considered out-flow model of water maser using data observed with VLA. They assumed the model that water masers were accelerated exponentially and expanded spherically. Based on this assumption, they showed a relationship between expansion velocities and the three-dimensional distances from the central star to the masers;

$$r = r_0 - \frac{1}{k} \ln \left(1 - \frac{v}{v_f} \right), \quad (3)$$

where r is three-dimensional distance from the central star to the maser, $k = 0.065 \text{ AU}^{-1}$, $r_0 = 1.5 \text{ AU}$ is the radius at which expansion velocities are zero, $v_f = 8.4 \text{ km s}^{-1}$ is the largest expansion velocity, and v is the expansion velocity of masers. By using their model, we can estimate the three-dimensional distance from central star to the maser. On the celestial plane, the difference of proper motion between the maser and the central star is 2.8 mas yr^{-1} . This corresponds to 1.8 km s^{-1} . The difference of the radial velocities is 2.2 km s^{-1} . From these, the expansion velocity is $v = \sqrt{1.8^2 + 2.2^2} = 2.8 \text{ km s}^{-1}$. From equation (3), we obtained the three-dimensional distance from central star to be 7.9 AU . This distance is smaller than the inner radius of the detected incomplete ring structure by Winnberg et al. (2008).

4. Discussion

4.1. Position on the PL-relation

The parallax 7.31 ± 0.50 mas obtained as above gives the distance modulus of -5.68 mag. We apply this to assume the absolute magnitude of RX Boo. For RX Boo Glass & van Leeuwen (2007) used the apparent K magnitude m_K of -1.85 mag based on the observation by Lloyd Evans and the parallax of 4.98 ± 0.64 mas derived from the revised Hipparcos Catalogue (van Leeuwen & Fantino 2005; van Leeuwen 2007). Their values gave the absolute magnitude M_K of $-8.36_{-0.30}^{+0.26}$ mag. Our new parallax gives M_K of $-7.53_{-0.15}^{+0.14}$. This magnitude may have also the probable error about 0.4 mag or less as indicated in Glass & van Leeuwen (2007).

The period of variable stars classified as semi-regular (SR) is difficult to determine precisely. In 1980s, Taylor (1987) reported the existence of two periods, 160.0 d and 302.0 d, for

RX Boo. Andronov & Kudashkina (1988) obtained several periods based on their observational results. In the General Catalogue of variable Stars (GCVS) by Samus et al. (2009) the period of 162.3 d is tabulated for RX Boo, although Glass & van Leeuwen (2007) used 340 d indicated in the former version of GCVS. The period of 162.3 d is based on Mattei et al. (1997). Mattei et al. (1997) give the period of 304.7 d together with 162.3 d adopted in GCVS. They have also suggested the existence of the third period of 2691.837 d without confirmation. A recent paper by Speil (2006) gives also the double-periodicity of 278.0 and 169.6 d. Because of the uncertainty of the period determination for the semiregular variables, it is difficult to judge which periods are the most essential to present the nature of the variability of RX Boo. At least, we accept the fact that the stellar variability show the double-periodic nature with the shorter period of 160 - 170 d and the longer one of 280 - 350 d. These early studies of periods of RX Boo are tabulated in table 4.

The period-luminosity relation is useful not only to estimate the distance of astronomical objects but also to study the stellar structure and pulsation properties. The above obtained M_K and the periods should be compared with the PL-relation of the long-period variables in our Galaxy and the Magellanic Clouds. Glass & van Leeuwen (2007) compared the period and M_K with the Period-Luminosity sequences originally found in the Magellanic Cloud by Wood (2000) and corrected by Ita et al. (2004). The relation for Miras and SRa stars is labeled as sequence C, and that for some of SRb as sequence C'. For the long period, RX Boo is found on sequence C, and on sequence C' for the short period. The fact indicates that both two periods of RX Boo look concerned with the basic properties of stellar structure not with any spontaneous occurrence. One of the periods corresponds to a definite mode of pulsation, and the other to another mode. The simultaneous enhancement of both modes may be evidence for the transient nature of RX Boo between the sequence C and C' stars.

4.2. *Stellar radius and temperature*

The revision of the parallax will yield the derivation of the revised physical parameters of the star. A thorough survey of late-type giants including RX Boo has been performed by Kučinskis et al. (2005). They discussed the Rosseland radius for a measure of the stellar radius. It is defined as the radius where the optical depth calculated by using the opacities with the Rosseland mean is equal to the unity. The radius is very similar to the radius where the total flux corresponds to that derived from the effective temperature of stellar atmospheres. For RX Boo, Kučinskis et al. (2005) used the angular diameter of the Rosseland radius, 18.87 ± 0.12 mas, based on the results in Perrin et al. (1998). The Rosseland radius of 278 solar radii is obtained by combining their radius and the present parallax. The estimated value of the radius should be increased from this when we adopt the uniform disk angular diameter of 21.0 ± 0.3 mas derived by Chagnon et al. (2002).

The stellar radius can be derived with another procedure that is based on the apparent

magnitude, the effective temperature of stellar atmosphere, and the parallax. In GCVS, the maximum and minimum V magnitude are tabulated as 6.43 and 9.1. We may assume the mean V magnitude of 7.8 from these values. Kučinskas et al. (2005) adopted V of 7.98 in their study. We may assume the mean V magnitude of 8.0 from the AAVSO results between 1987 and 2007 demonstrated in Winnberg et al. (2008). The results presented by AFOEV also show the mean V magnitude of about 8.0. After V magnitude of 8.0 is chosen, the color ($V - K$) of 9.85 is derived by using K magnitude tabulated in Glass & van Leeuwen (2007). We can obtain the bolometric correction of about -6.5 mag (Worthey & Lee 2011), and then we have the apparent bolometric magnitude m_{BOL} of 1.5 mag. Finally, we have M_{BOL} of -4.2 which gives the stellar luminosity of $3630 L_{\odot}$ or $\log(L/L_{\odot}) = 3.56$. When we use the effective temperature of 2750 K based on Worthey & Lee (2011), the radius of $266 R_{\odot}$ is obtained. The effective temperature of such a late M type stars is difficult to estimate from the study of stellar atmospheres. Aringer et al. (1999) have found that the effective temperature of semiregular variables is hotter than Mira stars. This result suggests that the effective temperature of RX Boo will be higher than the mean value for the late-type giants. Such a higher temperature yields smaller radius for this star. Further study on this problem will be interesting.

At present, we may suppose the radius of RX Boo of about $270 R_{\odot}$ based on the results obtained with two different procedure.

4.3. *Stellar mass and evolutionary status*

The radius of a pulsating star can be used to estimate the stellar mass when the characteristic period, the pulsation constant, Q is obtained from theoretical consideration. The detailed theoretical study on the radial pulsation of red giants performed by Xiong & Deng (2007) gives the period ratio and the characteristic period Q for various models. The period ratio of RX Boo is 0.61 for the results of Speil (2006) and 0.53 for those of Mattei et al. (1997). The theoretical ratio of the first overtone period P_{10} to the fundamental period P_{F} scatters for less massive and cool models. So it looks difficult to obtain precise results but the period ratio of 0.53 is preferable for the theoretical results. In their theoretical results, the characteristic period for the first overtone mode Q_{10} does not scatter even for luminous models. We may use Q_{10} of about 0.039 or $\log Q_{10} \simeq -1.41$ when we use their algebraic expression, even though the luminosity of RX Boo $\log(L/L_{\odot}) = 3.56$ exceeds the range of their calculation unfortunately. From the period-density relation,

$$Q_{10} = P_{10} \sqrt{M/R^3},$$

we obtain the mass of RX Boo of $1.13 M_{\odot}$. The mass estimated here will be increased when we adopt larger radius.

The luminosity and mass of RX Boo can be compared with the theoretical studies of AGB stars. A diagram titled as evolution in mass and luminosity for solar composition stars prepared by G. H. Bowen is presented in Wilson (2000). The diagram shows the rather schematic figure

of the evolutionary path on the $\log L$ - $\log M$ diagram. It indicates that first a star of intermediate mass evolves with the increase in the luminosity and almost constant mass, and then the mass decreases with high mass loss rate when the star reaches a critical luminosity. Such a critical mass-luminosity line is called as the cliff in her paper. The luminosity and mass obtained here for RX Boo indicate the star on the locus of evolutionary track for the initial mass of $1 M_{\odot}$ and before reaching the cliff. In Wilson's diagram, the mass loss rate is also indicated, and the rate of $10^{-8} \dot{M}$ is found for this position. The mass loss rate of $6 - 2 \times 10^{-7} M_{\odot} \text{ yr}^{-1}$ derived by Olofsson et al. (2002) and by Teyssier et al. (2006) does not coincide with the properties of RX Boo presented above.

Because the derived mass depends on the adequacy of our assumption that Q_{10} will be constant for cool and bright AGB stars, further examination on the stellar mass should be required.

5. Summary

We have measured annual parallax of the Semiregular variable RX Bootis by tracking a maser spot at $V_{\text{LSR}} = 3.2 \text{ km s}^{-1}$ for one year. The annual parallax is $7.31 \pm 0.50 \text{ mas}$, corresponding to the distance of $136_{-9}^{+10} \text{ pc}$. The luminosity by using the present parallax is $3630 L_{\odot}$ or $\log(L/L_{\odot}) = 3.56$. With this luminosity and latest periods, RX Boo is found on Sequences C and C' originally discovered on the period-luminosity diagram of the LMC. Based on the present results, we derived the stellar radius of about $270 R_{\odot}$. The mass of about $1 M_{\odot}$ is estimated from the radius and the theoretical pulsation properties. This mass and the luminosity indicate that RX Boo remains still at the slowly evolving phase based on the results of stellar evolution consideration. Such an estimate matches the comparatively small mass loss rate of this star. RX Boo seems to be before the phase of strong mass loss.

References

- Andronov, I. L., & Kudashkina, L. S. 1988, *Astronomische Nachrichten*, 309, 323
- Aringer, B., Höfner, S., Wiedemann, G., Hron, J., Jørgensen, U. G., Käufel, H. U., & Windsteig, W. 1999, *A&A*, 342, 799
- Bedding, T. R., & Zijlstra, A. A. 1998, *ApJL*, 506, L47
- Bedding, T. R., Zijlstra, A. A., Jones, A., & Foster, G. 1998, *MNRAS*, 301, 1073
- Boboltz, D. A., & Claussen, M. J. 2004, *Bulletin of the American Astronomical Society*, 36, 1357
- Cioni, M.-R. L., Marquette, J.-B., Loup, C., Azzopardi, M., Habing, H. J., Lasserre, T., & Lesquoy, E. 2001, *A&A*, 377, 945
- Chagnon, G., Mennesson, B., Perrin, G., Coudé du Foresto, V., Salomé, P., Bordé, P., Lacasse, M., & Traub, W. 2002, *AJ*, 124, 2821
- Dyck, H. M., Benson, J. A., van Belle, G. T., & Ridgway, S. T. 1996, *AJ*, 111, 1705
- Feast, M. W., Glass, I. S., Whitelock, P. A., & Catchpole, R. M. 1989, *MNRAS*, 241, 375

Glass, I. S., & Evans, T. L. 1981, *Nature*, 291, 303

Glass, I. S., & van Leeuwen, F. 2007, *MNRAS*, 378, 1543

Groenewegen, M. A. T., & Whitelock, P. A. 1996, *MNRAS*, 281, 1347

Hedden, J., Benson, P. J., Little-Marenin, I. R., & Cadmus, R. R. 1991, *Journal of the American Association of Variable Star Observers (JAAVSO)*, 20, 198

Honma, M., et al. 2007, *PASJ*, 59, 889

Honma, M., et al. 2008a, *PASJ*, 60, 935

Honma, M., Tamura, Y., & Reid, M. J. 2008b, *PASJ*, 60, 951

Ita, Y., et al. 2004, *MNRAS*, 353, 705

Jike, T., Fukuzaki, Y., Shibuya, K., Doi, K., Manabe, S., Jauncey, D. L. Nicolson, G. D., & McCulloch, P. M. 2005, *Polar Geoscience*, 18, 26

Knapp, G. R., Pourbaix, D., Platais, I., & Jorissen, A. 2003, *A&A*, 403, 993

Kobayashi, H., et al. 2003, *Astronomical Society of the Pacific Conference Series*, 306, 367

Kučinskas, A., Hauschildt, P. H., Ludwig, H.-G., Brott, I., Vansevičius, V., Lindegren, L., Tanabé, T., & Allard, F. 2005, *A&A*, 442, 281

Manabe, S., Yokoyama, K., & Sakai, S. 1991, *IERS Techn. Note*, 8, 61

Mattei, J. A., Foster, G., Hurwitz, L. A., Malatesta, K. H., Willson, L. A., & Mennessier, M. O. 1997, *Hipparcos - Venice '97*, 402, 269

Nakagawa, A., et al. 2008, *PASJ*, 60, 1013

Noda, S., et al. 2004, *MNRAS*, 348, 1120

Olofsson, H., González Delgado, D., Kerschbaum, F., & Schöier, F. L. 2002, *A&A*, 391, 1053

Perrin, G., Coudé du Foresto, V., Ridgway, S. T., Mariotti, J.-M., Traub, W. A., Carleton, N. P., & Lacasse, M. G. 1998, *A&A*, 331, 619

Perryman, M. A. C., et al. 1997, *A&A*, 323, L49

Samus, N. N., Durlevich, O. V., & et al. 2009, *VizieR Online Data Catalog*, 1, 2025

Shibata, K. M., Kamenno, S., Inoue, M., & Kobayashi, H. 1998, *IAU Colloq. 164: Radio Emission from Galactic and Extragalactic Compact Sources*, 144, 413

Speil, J. 2006, *Journal of the American Association of Variable Star Observers (JAAVSO)*, 35, 88

Szymczak, M., Le Squeren, A. M., Sivagnanam, P., Tran Minh, F., & Fournier, A. 1995, *A&A*, 297, 494

Taylor, M. D. 1987, *Journal of the British Astronomical Association*, 97, 277

Teyssier, D., Hernandez, R., Bujarrabal, V., Yoshida, H., & Phillips, T. G. 2006, *A&A*, 450, 167

van Belle, G. T., Thompson, R. R., & Creech-Eakman, M. J. 2002, *AJ*, 124, 1706

van Leeuwen, F. 2007, *A&A*, 474, 653

van Leeuwen, F., & Fantino, E. 2005, *A&A*, 439, 791

Vlemmings, W. H. T., & van Langevelde, H. J. 2007, *A&A*, 472, 547

Whitelock, P., & Feast, M. 2000, *MNRAS*, 319, 759

Whitelock, P. A., Feast, M. W., & van Leeuwen, F. 2008, *MNRAS*, 386, 313

Winnberg, A., Engels, D., Brand, J., Baldacci, L., & Walmsley, C. M. 2008, *A&A*, 482, 831

Wood, P. R. 2000, *Publications of the Astronomical Society of Australia*, 17, 18

Woodruff, H. C., Tuthill, P. G., Monnier, J. D., Ireland, M. J., Bedding, T. R., Lacour, S., Danchi, W. C., & Scholz, M. 2008, *ApJ*, 673, 418
Worthey, G., & Lee, H.-c. 2011, *ApJS*, 193, 1
Xiong, D. R., & Deng, L. 2007, *MNRAS*, 378, 1270
Yeşilyaprak, C., & Aslan, Z. 2004, *MNRAS*, 355, 601
Zijlstra, A. A., Bedding, T. R., & Mattei, J. A. 2002, *MNRAS*, 334, 498